

# Proceedings of the 11th International Conference on Structures in Fire



Editors: David Lange, Cristian Maluk, Kang Hai Tan, Dong Zhang, Yao Zhang,  
Julian Mendez Alvarez, Juan Hidalgo, Felix Wiesner, Martyn McLaggan,  
Abdulrahman Zaben, Wenxuan Wu, Hangyu Xu

**UQ Fire**



**THE UNIVERSITY  
OF QUEENSLAND  
AUSTRALIA**

CREATE CHANGE

**NETZSCH**  
Proven Excellence.

**afac** 

**omnii**  
Consulting Fire Engineers

**Proceedings of the 11<sup>th</sup>  
International  
Conference on  
Structures in Fire**

**Hosted by The University of Queensland**

Proceedings of the 11<sup>th</sup> International Conference on Structures in Fire  
(SiF 2020)

Hosted by The University of Queensland

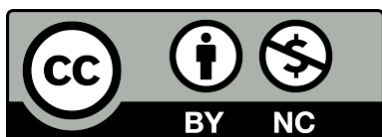
30 November to 2 December 2020

Editors: David Lange, Cristian Maluk, Kang Hai Tan, Dong Zhang, Yao Zhang, Julian Mendez Alvarez,  
Juan Hidalgo, Felix Wiesner, Martyn Mclaggan, Abdulrahman Zaben, Wenxuan Wu, Hangyu Xu

Published by The University of Queensland, Australia © 2020

ISBN: 978-1-74272-343-3

All articles included in this collection are published under a Creative Commons Attribution Non-  
Commercial (CC BY 4.0) License



**Sponsored by:**

**NETZSCH**

Proven Excellence.



**omnii**  
Consulting Fire Engineers

**Organised by:**

**UQ Fire**



CREATE CHANGE



## TABLE OF CONTENTS

Table of contents	v
Preface	xii
Committees	xiv
<b>Applications of structural fire engineering</b>	
A practical tool for evaluating fire induced failure probability of steel columns designed based on U.S. prescriptive standards <i>Ramla Qureshi; Ruben Van Coile; Danny Hopkin; Thomas Gernay; Negar Elhami Khorasani</i>	1
Fire performance of a steel open car park in the light of the recent development of the localised fire model "LOCAFI" <i>Mauro Sommavilla; Nicola Tondini</i>	12
The collapse of World Trade Center 7: revisited <i>Mhd Anwar Orabi; Liming Jiang; Asif Usmani; Jose L. Torero</i>	23
Steel sheet piles exposed to fire experimental tests and numerical modelling <i>Jean-Marc Franssen; João Martins</i>	34
Modelling concrete slabs subjected to localised fire action with OpenSees <i>Liming Jiang; Mhd Anwar Orabi; Jin Qiu; Asif Usmani</i>	46
A framework for reliability-based assessment of structures in post-fire conditions <i>Tom Molkens; Barbara Rossi</i>	55
Influence of time step on stability of the hybrid fire testing in a limited divergence zone <i>Bunthan Iea; Duc Toan Pham; Nicolas Pinoteau; Romain Mege; Jean-François Caron</i>	67
Real-time multi degrees of freedom hybrid fire testing using Pi control <i>Elke Mergny; Jean-Marc Franssen</i>	77
Lifetime economically optimum position of steel reinforcement in a concrete column exposed to natural fire <i>Shuna Ni; Ruben Van Coile; Negar Elhami Khorasani; Danny Hopkin; Thomas Gernay</i>	89

## Composite structures

- Evaluation of the fire performance of unprotected composite beams with fin-plate joints 101  
*N. Yotsumoto; T. Hirahisma; K. Toyoda*
- Effect of steel-fiber reinforced concrete on the fire resistance of concrete-filled steel tubular columns under simultaneous axial loading and double curvature bending 113  
*Takuya Kinoshita; Yusuke Shintani; Tomohito Okazaki; Toshihiko Nishimura; J Y Richard Liew*
- Applicability of the resistance integration method on bonded fasteners loaded in tension in uncracked concrete under ISO 834-1 fire 124  
*Omar Al-Mansouri; Romain Mège; Nicolas Pinoteau; Thierry Guillet; Sébastien Rémond*
- Bond behaviour of elliptical concrete-filled steel tubes after fire exposure 134  
*Tianyi Song; Xialu Liu; Kai Xiang*
- Bonding of grouted eccentric strands in duct at elevated temperatures 146  
*Xiqiang Wu; Francis Tat Kwong Au; Xinyan Huang*
- Experimental study on fire resistance of a full-scale composite floor assembly in a two-story steel framed building 158  
*Lisa Choe; Selvarajah Ramesh; Xu Dai; Matthew Hoehler; Matthew Bundy*
- The role of end conditions on the behaviour of steel-concrete composite beams in fire 171  
*Priya S. Natesh; Anil Agarwal*

## Concrete structures

- Effect of transverse and longitudinal confinement on the interlayer bond in 3D printed concrete at elevated temperatures: an experimental study 184  
*Antonio Cicione; Khanya Mazolwana; Jacques Kruger; Ricahrd Walls; Zara Sander; Gideon Van Zijl*
- Predicting the fire rating of cantilever slab-wall connection with post installed rebar 196  
*Hitesh Lakhani; Jatin Aggarwal; Jan Hofmann*
- Influence of spalling on the biaxial bending resistance of reinforced concrete columns exposed to fire 204  
*David L. Peña; Carmen Ibáñez; Vicente Alberó; Ana Espinós; Antonio Hospitaler; Manuel L. Romero*
- Effect of non-uniform heating and cooling on eccentrically loaded reinforced concrete columns 212  
*Jamie Maclean; Luke Bisby; Carmen Ibáñez*
- Bond behavior between reinforcing steel bars and concrete at elevated temperatures 222  
*Ira Banoth; Anil Agarwal*
- Post-earthquake fire assessment of reinforced concrete columns 230  
*Hemanth Kumar Chinthapalli; Anil Agarwal*

Damage assessment framework for tunnel structures subjected to fire <i>Nan Hua; Anthony Frederick Tessari; Negar Elhami Khorasani</i>	242
Comparative fire behavior of reinforced concrete beams made of different concrete strengths <i>Venkatesh Kodur; Srishti Banerji</i>	254
Modeling the structural behavior of reinforced concrete walls under ISO fire exposure <i>Mohsen Roosefid; Marie Helene Bonhomme; Pierre Pimienta</i>	262
Numerical investigation of the structural response of eccentrically loaded reinforced concrete columns exposed to non-uniform heating and cooling <i>Patrick Bamonte; Nataša Kalaba; Jamie Maclean; Luke Bisby</i>	271
Global resistance factor for the burnout resistance of concrete slabs exposed to parametric fires <i>Thomas Thienpont; Ruben Van Coile; Balsa Jovanovic; Wouter De Corte; Robby Caspeele</i>	282
Bond strength between steel reinforcement and RCA concrete at elevated temperatures <i>Md. Abu Yusuf; Salah Sarhat; Hamzeh Hajiloo; Mark F. Green</i>	293
Evaluation of expected damage costs from fire in concrete building structures <i>Shuna Ni; Thomas Gernay</i>	301
Spalling of geopolymer concrete in ring-restrained specimens under high temperatures <i>Mitsuo Ozawa; Hiroyuki Ikeya; Koji Harada; Hiroki Goda</i>	313
Generalized fragility curves for concrete columns exposed to fire through surrogate modelling <i>Ranjit Kumar Chaudhary; Balša Jovanović; Thomas Gernay; Ruben Van Coile</i>	322
Critical fibre dimensions for preventing spalling of ultra-high performance concrete at high temperature <i>Dong Zhang; Kang Hai Tan</i>	333
Probabilistic models for thermal properties of concrete <i>Balša Jovanović; Negar Elhami Khorasani; Thomas Thienpont; Ranjit Kumar Chaudhary; Ruben Van Coile</i>	342
Effect of steel fibers on fire endurance of extruded hollow-core slabs <i>Hang T N Nguyen; Kang Hai Tan</i>	353
<b>Experimental research and any other</b>	
Retrofitting of fire damaged RC columns <i>Hemanth Kumar Chinthapalli; M. Chellapandian; Anil Agarwal; Suriya Prakash</i>	363
Developing real-time hybrid simulation to capture column buckling in a steel frame under fire <i>Ramla K Qureshi; Negar Elhami Khorasani; Mettupalayam Sivaselvan</i>	374
Thermal response and capacity of beam end shear connections during a large compartment fire experiment <i>Xu Dai; Lisa Choe; Erica Fischer; Charles Clifton</i>	386

Experimental study of concrete elements subjected to travelling fires <i>Camilo Montoya; David Lange; Cristian Maluk; Juan P. Hidalgo</i>	398
Robust circle tracking for deflection measurements in structural fire experiments <i>Felix Wiesner; Luke Bisby</i>	410
Alkali-activated sprayed concrete as a fire protection coating for tunnels inner lining: proof-of-concept study on the heat transfer <i>Anna-Lena Hammer; Christian Rhein; Thomas Rengshausen; Markus Knobloch; Götz Vollmann; Markus Thewes</i>	418
Evaluation of measuring methods for water vapor pressure in concrete at elevated temperature <i>Ye Li; Kang Hai Tan</i>	430
Travelling fire in full scale experimental building subjected to open ventilation conditions <i>Ali Nadjai; Naveed Alam; Marion Charlier; Olivier Vassart; Xu Dai; Jean-Marc Franssen Johan Sjöström</i>	439
Shear resistance of sandwich panel connection to the substructure at elevated temperature <i>Kamila Cábová; Marsel Garifullin; Ashkan Shoushtarian Mofrad; František Wald; Kristo Mela; Yvonne Ciupack</i>	451
Near-limit burning of timber material under irradiation-assisted smoldering <i>Shaorun Lin; Xinyan Huang</i>	458
Rotational ductility of steel web-flange splice connections in fire <i>Paul Akagwu; Faris Ali; Ali Nadjai</i>	468
Fire experiments inside a very large and open-plan compartment: x-TWO <i>Mohammad Heidari; Egle Rackauskaite; Matthew Bonner; Eirik Christensen; Sébastien Morat; Harry Mitchell Panos Kotsovinos; Piotr Turkowski; Wojciech Wegrzynski; Piotr Tofilo; Guillermo Rein</i>	479
Assessment of a fire damaged concrete overpass: the Verona bus crash case study <i>Roberto Felicetti</i>	492
<b>Numerical modelling</b>	
Simple calculation method for the temperature profile in a circular concrete filled steel tubular column <i>Yusuke Shintani; Takuya Kinoshita; Tomohito Okazaki; Toshihiko Nishimura; Tamotsu Takao</i>	504
Simulation of pyrolysis and combustion of pine wood using two-step reaction scheme <i>Dharmit Nakrani; Tejas Wani; Gaurav Srivastava</i>	515
A simplified representation of travelling fire development in large compartment using CFD analyses <i>Marion Charlier; Olivier Vassart; Xu Dai; Stephen Welch; Johan Sjöström; Johan Anderson Ali Nadjai</i>	526

Disproportionate collapse of steel-framed gravity buildings under fires with a cooling phase <i>Jian Jiang; Bowen Wang; Wenyu Cai; Guo-Qiang Li; Wei Chen; Jihong Ye</i>	537
Simple structural models for computational analysis of restrained columns under fire conditions <i>Pedro Dias Simão; João Paulo C. Rodrigues</i>	543
A static solver for hybrid fire simulation based on model reduction and dynamic relaxation <i>Patrick. Covi; Giuseppe Abbiati; Nicola Tondini; Oreste Salvatore Bursi; Bozidar Stojadinovic</i>	556
A thermo-mechanical stochastic damage perspective for concrete at elevated temperatures <i>Hao Zhou</i>	567
Linked CFD-thermo-mechanical simulation for virtual horizontal furnace <i>Stanislav Šulc; Kamila Cábová; Filip Zeman; Jakub Šejna; Vít Šmilauer; František Wald</i>	579
AI modelling & mapping functions: a cognitive, physics-guided, simulation-free and instantaneous approach to fire evaluation <i>M Z Naser; Haley Hostetter; Aditya Daware</i>	590
A numerical investigation of 3D structural behavior for steel-composite structures under various travelling fire scenarios <i>Zhuojun Nan; Xu Dai; Haimin Chen; Stephen Welch; Asif Usmani</i>	599
An improved implicit analysis method to model transient strain of high-strength concrete during unloading at elevated temperatures <i>Shan Li; J Y Richard Liew; Ming-Xiang Xiong</i>	611
The behaviour of bridge decks due to fire induced thermal expansion of protected stays cables <i>Panagiotis Kotsovinos; Egle Rackauskaite; Ryan Judge; Graeme Flint; Peter Woodburn</i>	622
Modelling Grenfell disaster: interactions between facades and apartments <i>Eric Guillaume; Virginie Dréan; Bertrand Girardin; Talal Fateh</i>	627
<b>Steel structures</b>	
Studies on bending strength and collapse temperature of a steel beam considering effects of steel strain rate and heating rate at elevated temperatures <i>Fuimnobu Ozaki; Takumi Umemura</i>	639
Experimental and numerical-analytical study on structural behavior of steel frames based on small-scale fire tests <i>Akinobu Takada; Tomohito Okazaki; Mami Saito</i>	650
Investigation of the performance of a novel ductile connection within bare-steel and composite frames in fire <i>Yu Liu; Shan-Shan Huang; Ian Burgess</i>	662
Behaviour of axially compressed angles and built-up steel members at elevated temperature <i>Luca Possidente; Nicola Tondini; Jean-Marc Battini</i>	673

Stability check of web-tapered steel beam-columns in fire <i>Elio Maia; Paulo Vila Real; Nuno Lopes; Carlos Couto</i>	685
Post-fire mechanical properties of TMCP high strength structural steel <i>Lin-Xin Song; Guo-Qiang Li; Qing Xu</i>	697
Prediction of fracture behavior for high-strength steel bolts at elevated temperatures <i>Wenyu Cai; Jian Jiang; Guo-Qiang Li</i>	708
New methodology for the calculations on steel columns with thermal gradients in contact with brick walls <i>António Moura Correia; João Paulo Rodrigues; Venkatesh Kodur</i>	715
OpenSees simulation of the collapse of Plasco tower in fire <i>Ramakanth Veera Venkata Domada; Aatif Ali Khan; Mustesin Ali Khan; Asif Usmani</i>	727
Fire resistance of stainless steel slender elliptical hollow section beam-columns <i>Flávio Arrais; Nuno Lopes; Paulo Vila Real</i>	739
Material properties of structural, high strength and very high strength steels for post-fire assessment of existing structures <i>Tom Molkens; Katherine A. Cashell; Barbara Rossi</i>	751
Fire fragility curves for steel pipe-racks exposed to localised fires <i>Jérôme Randaxhe; Olivier Vassart; Nicola Tondini</i>	763
A novel approach to model the thermal and physical behaviour of swelling intumescent coatings exposed to fire <i>Andrea Lucherini; Juan P. Hidalgo; Jose L. Torero; Cristian Maluk</i>	775
Experimental study of unloaded structural steel stay-cables under fire exposure <i>Benjamin Nicoletta; Scott Watson; Bronwyn Chorlton; John Gales; Panagiotis Kotsovinos</i>	783
Experimental investigation of the behavior of martensitic high-strength steels at elevated temperature <i>Xia Yan; Yu Xia; Hannah B. Blum; Thomas Gernay</i>	791
Effect of transient creep on stability of steel columns exposed to fire <i>Venkatesh Kodur; Svetha Venkatachari</i>	803
<b>Timber structures</b>	
Compressive strength and MoE of solid softwood at elevated temperatures <i>Abdulrahman Zaben; David Lange; Cristian Maluk</i>	811
A method for determining time equivalence for compartments with exposed mass timber, using iterative parametric fire curves <i>David Barber; Robert Dixon; Egle Rackauskaite; Khai Looi</i>	818

Calibration of a coupled post-flashover fire and pyrolysis model for determining char depth in mass timber enclosures <i>Colleen Wade; Danny Hopkin; Michael Spearpoint; Charles Fleischmann</i>	830
The behaviour of timber in fire including the decay phase - charring rates, char recession and smouldering <i>Joachim Schmid; Antonio Totaro; Andrea Frangi</i>	842
Design of timber-concrete composite floors for fire <i>Erica C. Fischer; Annabel B. Shephard; Arijit Sinha; Andre R. Barbosa</i>	852
Proposal for stress-strain constitutive models for laminated bamboo at elevated temperatures <i>Mateo Gutierrez Gonzalez; Cristian Maluk</i>	859
The use of research for the explicit consideration of self- extinction in the design of timber structures <i>Juan Cuevas; Cristian Maluk</i>	866
Fire performance of moment-resisting concealed timber connections reinforced with self-tapping screws <i>Oluwamuyiwa Okunrounmu; Osama (Sam) Salem; George Hadjisophocleous</i>	879
Deformation behaviour and failure time of glued laminated timber columns in fire <i>Takeo Hirashima; Heisuke Yamashita; Shungo Ishi; Tatsuki Igarashi; Shigeaki Baba; Tomoyuki Someya</i>	890
Comparative study on the fire behaviour of fire-rated gypsum plasterboards vs. thin intumescent coatings used in mass timber structures <i>Ambrosine Hartl; Qazi Samia Razzaque; Andrea Lucherini; Cristian Maluk</i>	901
The response of exposed timber in open plan compartment fires and its impact on the fire dynamics <i>Sam Nothard; David Lange; Juan P. Hidalgo; Vinny Gupta; Martyn S. McLaggan</i>	911

## **FIRE PERFORMANCE OF A STEEL OPEN CAR PARK IN THE LIGHT OF THE RECENT DEVELOPMENT OF THE LOCALISED FIRE MODEL “LOCAFI”**

Mauro Sommavilla<sup>1</sup>, Nicola Tondini<sup>2</sup>

### **ABSTRACT**

The paper presents the results of a comprehensive finite element thermo-mechanical analysis conducted on a steel open car park subjected to localised fires. In particular, the LOCAFI model, a localised fire model recently developed in a European research project to estimate the radiative heat flux received by vertical members, was exploited to evaluate the fire performance of bare steel columns under the typical fire scenario of 4 vehicles burning around a column. The car park, to be built in Italy, was designed according to the Italian Building Code and the Eurocodes with steel grade S460M. Different column profiles were selected in order to optimise the structural fire performance, structural weight and related costs. The parametric analysis showed that, for this fire scenario and the selected profiles, the LOCAFI model was not the major governing factor of the column collapse. Indeed, when collapse occurred, it was mainly caused by material fracture in the column element just below the slab and subjected to the Hasemi model. As a result, it was observed that cross sections with thicker flanges and webs, i.e. HE of the M series are to be preferred with respect to cross sections with same area but higher inertia such as HE of the B series, that are characterised by thinner flanges and webs. Finally, no composite action and fireproofing are potentially needed for the vertical members by accounting for a profile with an adequate low section factor and higher strength, e.g. in this specific case an HE 260 M series S460M quality.

**Keywords:** Localised fires; LOCAFI model, steel structures; open car park; finite element modelling

### **1 INTRODUCTION**

In the framework of the Fire Safety Engineering (FSE) approach, the fire behaviour of steel open car parks exposed to localised fires has been widely investigated in the last twenty years for which natural fire curves and fire scenarios have been derived. Full-scale tests were performed in France in the late ‘90s and recommendations about the rate of heat release (RHR) of typical Class 3 cars and commercial vehicles to be adopted in design are now available [1]<sup>3</sup>. Analytical models describing the effects of localised fires were included in the structural Eurocode EN1991-1-2 [1], i.e. Hasemi and Heskestad correlations. However, they have limited field of applicability, e.g. the Hasemi model is valid only for flame impacting the ceiling and it is typically employed for horizontal structural members located at the ceiling level, whereas the Heskestad model may be applied to vertical elements fully engulfed into the localised fire. Due to the absence in the code of a suitable model able to provide the thermal action on vertical members external to the fire, safe assumptions are usually taken. For instance, one common assumption is to take the heat flux computed at the top of the column by means of the Hasemi model and to apply it to all column cross sections or is to

---

<sup>1</sup> Senior Engineer, Arcelormittal Steligenca Italy  
e-mail: [mauro.sommavilla@arcelormittal.com](mailto:mauro.sommavilla@arcelormittal.com)

<sup>2</sup> Assistant Professor, Department of Civil, Environmental and Mechanical Engineering, University of Trento, Italy  
e-mail: [nicola.tondini@unitn.it](mailto:nicola.tondini@unitn.it), ORCID: <https://orcid.org/0000-0003-2602-6121>

It worth mentioning that a major event that occurred at the Liverpool Echo Arena car park fire that destroyed 1400 vehicles in 2018 was not in line with the proposed fire scenarios.

compute the Hasemi heat flux at each column cross section by using in the model correlation the height of the considered cross section, as indicated in the French guidelines [3]. Computational Fluid Dynamics can be a viable option but it is still rather computationally demanding and its use is not straightforward for engineers with typical structural background [4]. Therefore, by applying simplified and safe assumptions, the most severe scenario for the columns generally leads to the design of either fireproofed columns or steel-concrete composite columns (partially encased H-sections or concrete filled tubes) hindering the use of potentially more economical compact bare steel elements. This increases the costs of application and of maintenance, in the first case, or the complexity of joint detailing between the composite column and the unprotected steel-composite I-beams, in the second one. In the last few years, to overcome the lack of a simplified method that covers the computation of the radiative heat flux received by a column outside a localised fire, comprehensive research on localised fires at European level has been done [5,6] and it has led to the development of an analytical model [7], the LOCAFI model, able to predict the radiative heat flux in space and in time emitted by a fire of conical shape to vertical members exposed to localised fires. The LOCAFI model was implemented in the thermo-mechanical software SAFIR [8] that was thoroughly used in this work.

## 2 DESCRIPTION OF THE CASE STUDY

This work describes a detailed numerical investigation of an unprotected steel open car park to be built in Italy (see Figure 1), subjected to a fire scenario relevant for the column, i.e. 3 Class 3 vehicles and 1 commercial vehicle around it, as depicted in Figure 2a. This fire scenario is included in the Italian Fire Prevention Code [9] and others code in Europe, e.g. France [1]. The rate of heat release (RHR) is shown in Figure 2b, where Car 3 corresponds to the commercial vehicle. This fire scenario can be seen as four localised fires, which surround the column, but they do not engulf it. In more detail, the car park will be realised in the area of Turin. The structure is a 3 to 4-storey split-levels car park of dimensions 48 m x 40 m x 9/12 m (interstorey height = 3 m) with 16-m long IPE 500 steel-concrete composite beams and 220-mm deep steel decking spanning transversally over 5-m long beams and directly connected to the beam web by means of appropriate connectors so-called “wings”. In the transverse direction, between each column HE 120 B 5-m long profiles were employed. To minimise the impact on the structural weight the use of fine grain steel S460M according to EN10025-4:2019 was foreseen for both beams and columns. Concrete of class C35/45 inside the ribs and over the upper beam flange (plain slab of 8/10cm) was employed. Joints between columns and beams are pinned and horizontal loads are withstood either by appropriate steel bracings or concrete walls. The live load was taken equal to 2.5 kN/m<sup>2</sup>. The car park was designed in accordance with the Italian Building Code and the relevant parts of the Eurocodes.

In the original project, partially encased columns were envisaged, which were composed of an HE 260 A S355 with 8 additional  $\phi = 22$  mm reinforcement bars and concrete strength class C35/40 that filled the steel section between the two flanges. However, it was decided to also investigate a different solution by considering bare steel columns. In this respect, different profiles were considered in order to analyse their performance under the selected fire scenario and they are reported in Table 1. It is possible to observe that the utilisation ratio  $\mu$  is in the order of 15%-20%; thus, about half of the maximum suggested by the French Guidelines [3], i.e. 35%. These  $\mu$  values are due to the adopted philosophy that aims at the column overdesign to avoid fireproofing or a composite solution. Indeed, the partially encased solution would have entailed a higher utilisation ratio equal to 29%. Moreover, it is worth presenting the selection criteria of the column profiles. For instance, let us consider an HE 260 M and an HE 450 B. They have basically the same cross-sectional area (and consequently weight per unit length); therefore, the axial resistance  $N_{pl,Rd}$  is pretty much the same. However, they differ in terms flexural properties for which the HE 450 B profile has more favourable properties by having larger height and width, which in turn entails thinner thicknesses of the flanges and the web with respect to the HE 260 M. Thus, if the axial force is governing, as it is case because, apart from bending moments caused by second order effects, the columns are predominantly axially loaded due to the pinned connections and an HE 260 M should then exhibit a more favourable behaviour since it has a smaller section factor. Similar observations can be made for the HE 240 M and the HD 320x158.

Moreover, an HP 320x184 was also selected. It has an increased cross-sectional area ( $A = 234 \text{ cm}^2$ ) as well as enhanced flexural properties with respect to an equivalent HE 280 M profile ( $A = 240.2 \text{ cm}^2$ ), by keeping at the same a reasonable size, with respect to an equivalent HE 500 B profile ( $A = 238.6 \text{ cm}^2$ ), that it is important for a car park in order to maximise the available space for the parking spots.

Table 1. Column profiles

Profile	h (mm)	b (mm)	t <sub>w</sub> (mm)	t <sub>f</sub> (mm)	A (cm <sup>2</sup> )	I <sub>y</sub> (cm <sup>4</sup> )	I <sub>z</sub> (cm <sup>4</sup> )	G (kg/m)	Section factor (m <sup>-1</sup> )	N <sub>Ed</sub> /N <sub>pl</sub> (-)	λ <sub>y</sub> (-)	λ <sub>z</sub> (-)
HE 240 M	270	248	18	32	199.6	24290	8153	157	73	0.192	0.41	0.70
HE 260 M	290	268	18	32.5	219.6	31310	10450	172	72	0.174	0.37	0.65
HE 450 B	450	300	14	26	218.0	79890	11720	171	93	0.176	0.23	0.61
HD 320x158	330	303	14.5	25.5	201.2	39640	11840	158	89	0.190	0.32	0.58
HP 320x184	329	317	25	25	234.5	42340	13330	184	78	0.163	0.33	0.59

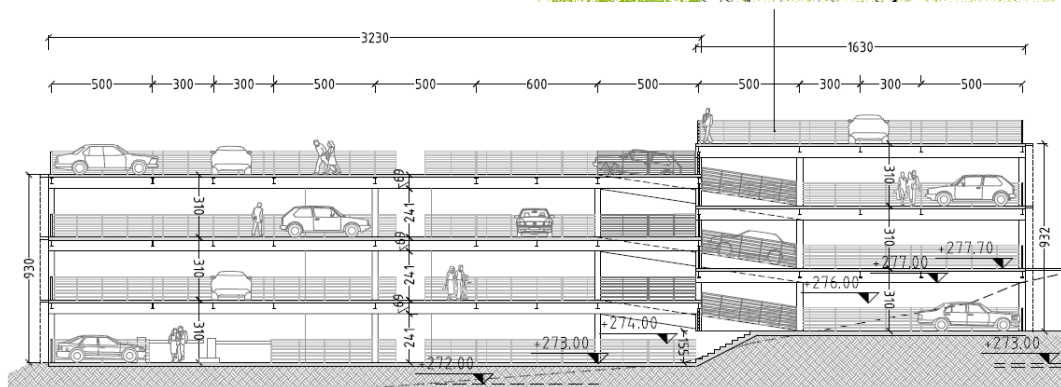


Figure 1 – Layout of the car park. Dimensions in cm.

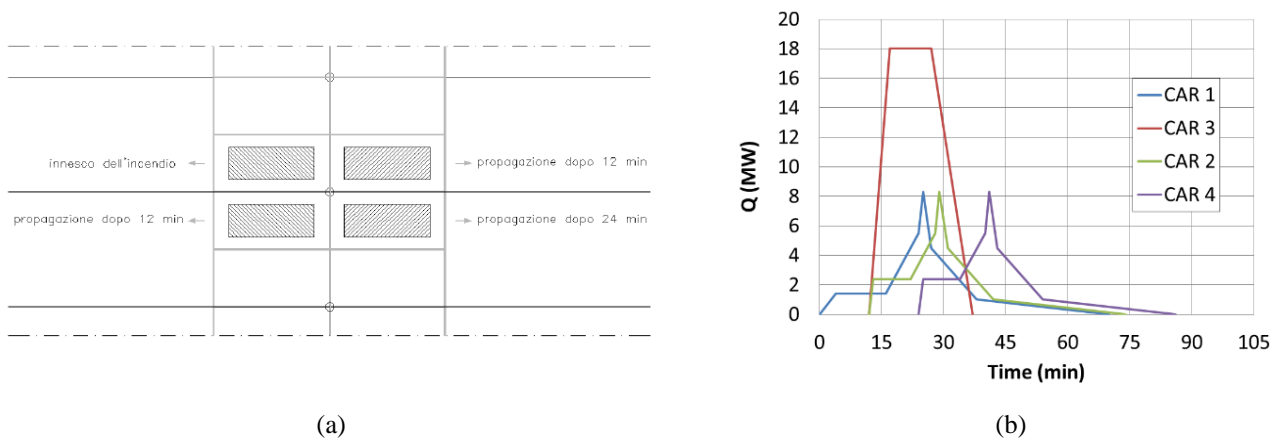


Figure 2 – a) Selected fire scenario according to the Italian Fire Prevention Code [9] and b) RHR of a 4-car scenario.

### 3 LOCAFI MODEL

Localised fires result from a liquid or solid fuel burning on a limited surface. Several models are available in literature to study localised fires and they can be classified among field/computational fluid dynamics (CFD) models and empirical/analytical models. Tondini et al. [7] showed how the analytical LOCAFI model compared with CFD models to predict the radiative heat flux emitted from localised fires and how it fared against experimental measurements. Among empirical/analytical models, solid flame models adopt a specific shape for the flame geometry, that may be a cylinder, an elliptical cylinder or a cone. These models consider that the radiative heat fluxes are emitted from the surfaces of the solid representing the fire and that the radiative heat flux received by an external element is the sum of the radiative heat fluxes emitted from each surface based on the computation of the configuration factor, which may be done analytically and/or numerically depending on the flame shape assumption. In the framework of this research, a solid flame model is adopted with the use of the LOCAFI model developed within the European LOCAFI Project. This model was developed and calibrated based on experimental tests and CFD numerical analyses [7]. A brief description is summarized herein.

The LOCAFI model represents the localised fire with a conical shape, as depicted in Figure 3. It means that the fuel is distributed in such a way that an equivalent circular representation of its distribution is still a reasonable assumption, i.e. when the ratio of the two sides of a hypothetical rectangular distribution is not greater than two. It has to be noted that LOCAFI model neglects wind effects, as it was done in this work. The fire model relies on the existing localised fire correlations provided in Annex C of EN1991-2 [2]. Thus, the length of the flame is defined in Equation (1) as a function of the fire diameter  $D$  and the rate of heat release  $Q$ .

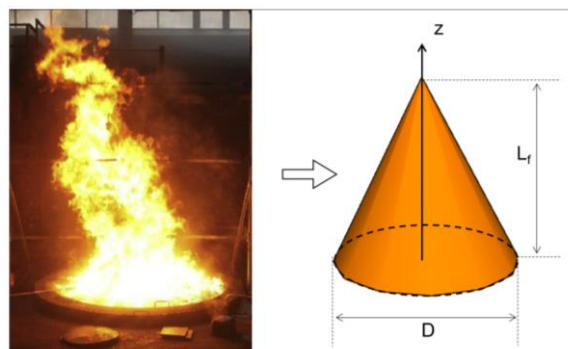


Figure 3. Solid flame modelled with conical shape in the LOCAFI model.

$$L_f = -1.02D + 0.0148Q^{2/5} \quad (1)$$

where  $D$  is the diameter (or its equivalent) of the localised fire (m) and  $Q$  is the RHR (W). The temperature along the vertical flame axis can be expressed with Equation (2) as a function of the height  $z$

$$T(z) = 20 + 0.25Q_c^{2/3} (z - z_0)^{-5/3} \leq 900 \quad (2)$$

$$z_0 = -1.02D + 0.00524Q^{2/5}$$

where  $T$  is the temperature ( $^{\circ}\text{C}$ ) along the centreline of the localised fire,  $Q_c$  is the convective part of the RHR  $Q$  in (W) taken as 0.8 times the RHR,  $z$  is the height along the fire centreline (m) and  $z_0$  is the virtual origin (m) and  $D$  is the diameter (or its equivalent) of the localised fire (m).

Once a localised fire is defined with a conical shape and a temperature evolution along the flame axis, incident radiative heat fluxes can be computed for any external element considered. Equation (3) defines the incident radiative heat flux  $\dot{q}_{inc.A \rightarrow B}^{\prime\prime}$  emitted by a surface A and received by a surface B.

$$\dot{q}_{inc.A \rightarrow B}^{\prime\prime} = \phi_{A \rightarrow B} \varepsilon_A \sigma (T_A + 273.15)^4 \quad (3)$$

Where  $\phi_{A \rightarrow B}$  is the configuration factor,  $\varepsilon_A$  is the emissivity of surface A,  $\sigma$  is the Stefan-Boltzmann constant ( $\text{W}/\text{m}^2\text{K}^4$ ) and  $T_A$  the temperature ( $^{\circ}\text{C}$ ) of surface A. The surface A is an element discretising the conical fire and the surface B is an element discretising the structural steel members. The emissivity of the flame  $\varepsilon_A$ , or  $\varepsilon_f$ , is conservatively taken equal to 1. The configuration factor can be determined analytically, if available, otherwise through numerical integration. In this work, the model implemented in SAFIR is based on numerical integration of the configuration factor. It discretizes the surfaces of the fire and the member with small elements. The temperature of each slice is calculated with Equation (2), by considering its average height. Steel members are represented with their actual cross section and shadows effects are considered. As explained in Section 4, the columns are modelled with beam elements with two points of integration each. At each integration point a 2D thermal analysis is performed with thermal boundary conditions that are representative of the position of the structural element with respect to the localised fire (or fires). In fact, SAFIR is able to compute at each time step and for each finite element located on the border of the cross section an incident radiative heat flux, which is calculated by summing all the radiative heat fluxes emitted by the surfaces discretizing the fire (or fires) and visible by the element according to a numerical procedure. Then, the net heat flux is expressed as the difference between the absorbed radiative heat flux and the heat fluxes reemitted by the surface B through radiation and convection at ambient temperature.

#### 4 NUMERICAL MODELLING

The numerical was developed with the thermo-mechanical software SAFIR [8]. A 3D FE model of half of the ground floor (48 m x 20 m x 3 m) was developed with the steel beams and columns modelled with Bernoulli beam elements and the concrete slab with quadrangular shell elements, as illustrated in Figure 4. Since the columns were continuous, the ones above the floor under study were also modelled and kept cold. Each exposed column was divided into 6 finite elements, with the top one just below the slab subjected to the Hasemi model, whilst the other five subjected to the LOCAFI model. The beams and the slab were subjected to the Hasemi model. Typically, this is a conservative assumption since the flame does not impact the ceiling during the whole duration of the fire scenario. The selected fire scenario of the 4 vehicles burning around one column described in Section 2 was included in SAFIR. The parking spots 2.5 m x 5 m were defined as equivalent circular areas centred at the middle of the parking and whose diameter was taken equal to 3.91 m. The thermal and mechanical material properties were selected according to the relevant fire parts of the Eurocodes. Partial reversibility of the steel strength was considered when the steel temperature exceeded  $600^{\circ}\text{C}$  by allowing for a loss of  $0.3 \text{ MPa}/^{\circ}\text{C}$ . For the concrete slab a bi-axial plane stress element that included the explicit transient creep strain model developed was employed [10]. The concrete model is calibrated on the EN 1992-1-2 model and it is able to take into account the non-reversibility of transient creep strain when the stress and/or the temperature decrease. Thus, the use of an explicit transient creep model allowed a more accurate analysis. Plasticity is based on a Drucker-Prager

yield function in compression and a Rankine cut off in tension. Compressive strength equal to 35 MPa was considered. The fracture energy, that was set to approximate the tension-stiffening effect, was taken as 1500 N/m<sup>2</sup>. This value was chosen based on the considerations made by Gernay et al. [11] to have a more robust numerical simulation. In this respect, the characteristic concrete tensile strength was lowered from 2.2 MPa, typical of a C35/40 concrete strength class, to 0.5 MPa. The other material parameters were considered as default values [8]. Concrete degradation at elevated temperature followed the EN 1992-1-2 provisions for siliceous aggregates. In the thermal analysis, the beam elements representing the IPE 500 were modelled with the slab on top of them only for thermal purposes as the slab acts as heat sink, as shown in Figure 4b, because in the mechanical analysis the slab was modelled with shell elements. Moreover, since the rib depth of the profiled steel sheet was significant (220 mm), in order to better model the slab, the ribs were represented by means of beam elements spanning transversely with section shown in Figure 4c, where only the rib is acting in the mechanical model, whereas the slab on the top was exploited only for the thermal analysis. Distributed loads were applied to the slab and point loads were applied at the top of the columns to simulate the load coming from the upper floors. After a sensitivity analysis on the mesh, the mechanical model was composed of 4581 nodes, 2347 beam elements and 1764 shell elements.

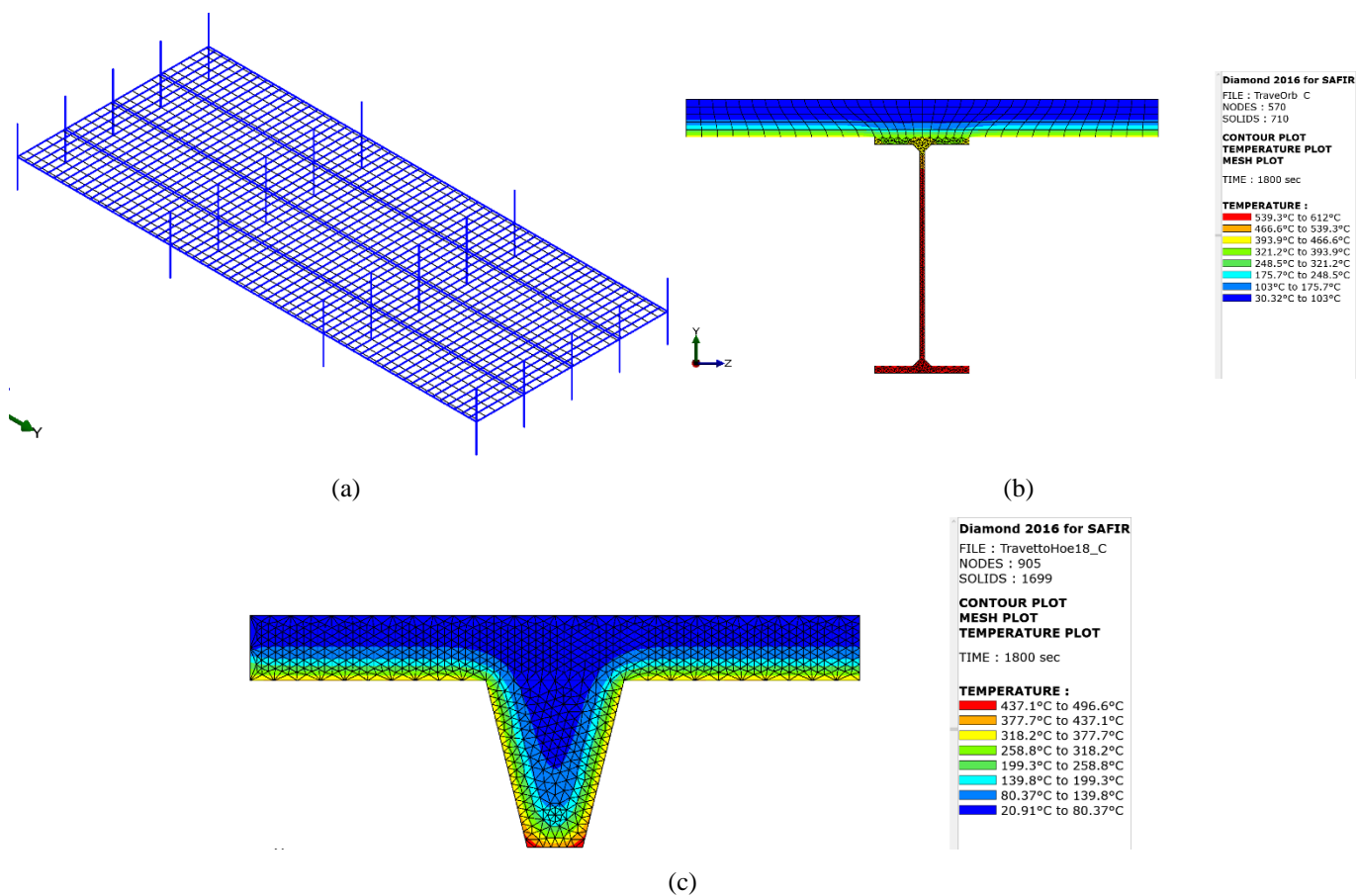


Figure 4. a) 3D finite element model; b) main beam modelling; c) slab rib modelling.

## 5 RESULTS AND DISCUSSION

The results of the thermo-mechanical analyses will mainly focus on the column surrounded by the burning vehicles since it is the objective of this work to investigate its fire behaviour. Moreover, it will be shown that the structural fire performance of the car park was governed by the column profile choice and failure, if it occurred, was indeed due to the loss of load-bearing capacity of the column.

### 5.1 Thermal analysis

The results of the thermal analysis relative to the selected columns are illustrated in Figure 5 and Figure 6. In particular, in Figure 5 the temperature distributions after 30 min of exposure to the fire scenario for three profiles (HE 260 M, HE 450 B, HP 320x184) are shown both for the Hasemi exposed element below the ceiling and for the LOCAFI most thermally impacted element at about 70 cm from the ground. It is possible to observe that, the Hasemi model is much more demanding in terms of thermal attack than the LOCAFI model. In fact, it causes peak steel temperatures in the order of 800-850°C. However, the temperature distributions in the three cross sections is markedly different (see Figure 5a, c and e). If we look at Figure 5c relative to HE 450 B, the entire web, i.e. about  $\frac{1}{4}$  of the entire cross-sectional area, is at temperatures higher than 800°C, which corresponds to a steel retention factor for the effective yield strength  $k_{y\theta} \leq 0.11$  [12]. Now, for the HE 450 B profile, as shown in Table 1, the utilisation ratio is 0.176 and this data already provides a hint that an HE 450 B may not be enough to support the applied axial load under the considered fire scenario. In this respect, the average temperature of the cross section after 30 min is beyond 750°C, which implies  $k_{y\theta} < 0.17$ . Conversely, looking at Figure 5a relative to the HE 260 M, which has about the same cross-sectional area as the HE 450 B, one may observe that, as expected, the temperature field is characterised by lower temperatures, with only about half of the web characterised by temperatures higher than 780°C. Moreover, the average section temperature can be roughly estimated in a value below 750°C; thus  $k_{y\theta} > 0.17$  and being  $\mu = 0.174$  this profile may have enough strength to survive the fire. The temperature field of the HP 320x184 is more uniform since the web and the flanges have the same thickness (Figure 5e) and similarly to the HE 260 M the average temperature in the cross section is less than 750°C with a utilisation ratio equal to 0.163. Figure 6a and b show the evolution in time of the temperature in the flange and in the web for each profile under the Hasemi model. It is possible to note that the HE 240 M and the HE 260 M have very similar temperature evolutions, which is consistent with their respective section factors and geometries, as shown in Table 1. However, the HE 240 M has a cross-sectional area, which is 10% less than the HE 260 M, and this may be affect the ability of the profile to sustain the applied loads under the fire scenario.

As expected, the LOCAFI model caused a significant non-uniform temperature distribution in the cross sections and along the member. Here, only the most heated cross sections are shown. In particular, Figure 5b, d and f highlight that at 30 min, a time that corresponds to all 4 vehicles burning (see Figure 2b), one flange corner is hotter than the rest of the cross section. Indeed, that part of the cross section is oriented towards the burning commercial vehicle that produces higher heat fluxes. However, peak temperatures lie under 500°C (see also Figure 6c) with most of the cross section being below 400°C, that is the temperature at which  $k_{y\theta}$  starts to decrease below 1.0. Therefore, the thermal impact of the LOCAFI model, despite causing thermal bowing and enhancing second order effects, should not govern the possible failure of the selected profiles. In sum, by analysing the results of the thermal analysis, a loss of the cross-section axial resistance of the column element subjected to the Hasemi model seems the main factor that can lead to the structural failure of the column.

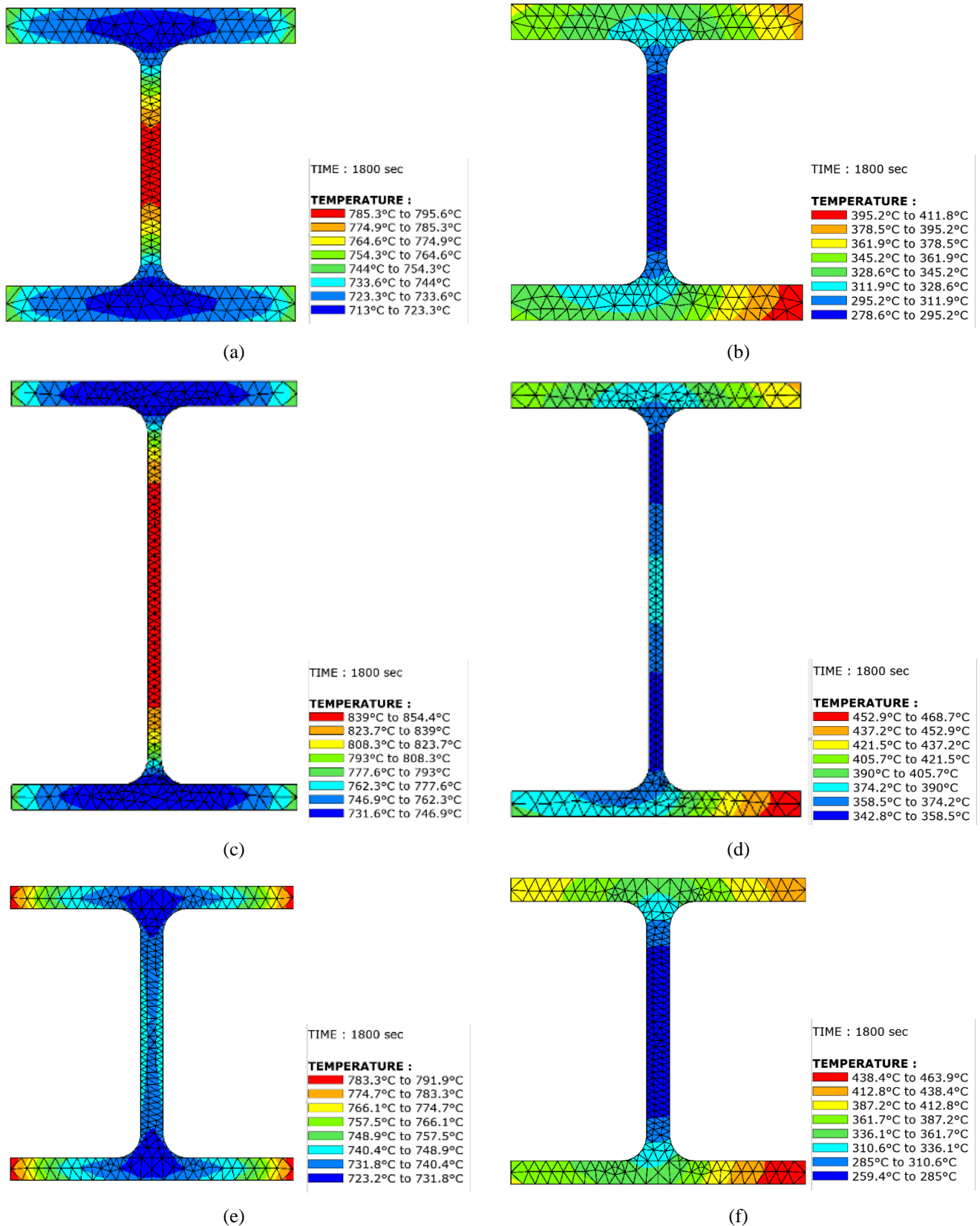


Figure 5. Column thermal analysis at 30 min: a) Hasemi HE 260 M; b) LOCAFI HE 260 M; c) Hasemi HE 450 B; d) LOCAFI HE 450 B; e) Hasemi HP 320x184; f) LOCAFI HP 320x184.

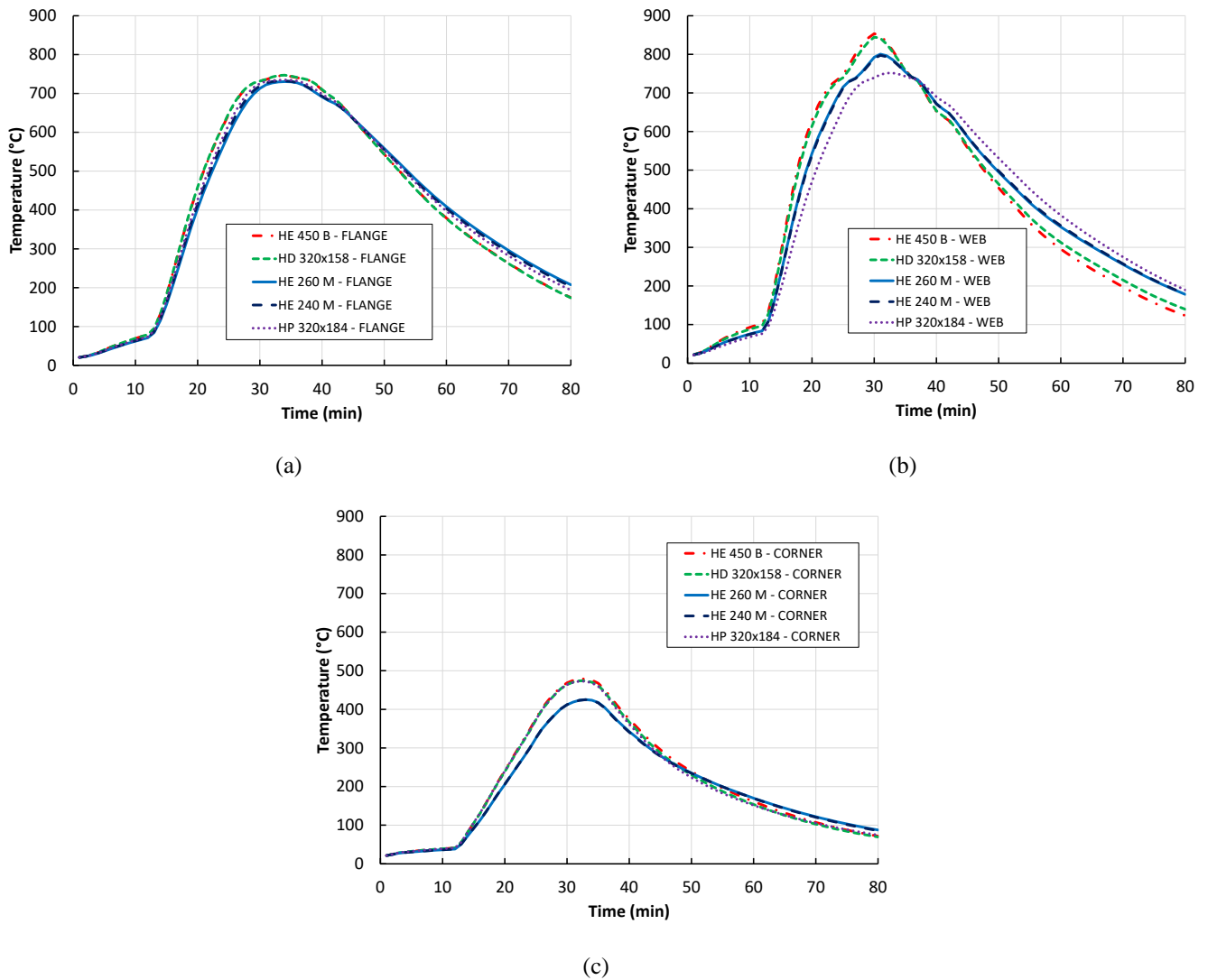


Figure 6. Column thermal analysis: a) Hasemi flange temperature; b) Hasemi web temperature; c) LOCAFI maximum temperature in the cross sections.

## 5.2 Mechanical analysis

All five mechanical responses were run based on the outcomes of the thermal analysis. Three out of five analyses did not converge and structural failure of the column was observed. Indeed, as hinted before by looking at thermal analysis results, the top column element heated by the Hasemi model was the cause of collapse owing to loss of load-bearing capacity under the applied forces, as shown in Figure 7 for the HE 450 B case. The analyses with the HE 260 M and the HP 320x184 profiles survived the whole duration of the fire with maximum vertical displacement of the slab above the commercial vehicle being in the order of 50 cm, as illustrated in Figure 8. Indeed, based on the thermo-mechanical outcomes that exploit the new available LOCAFI fire model that allows for the prediction of the heat fluxes along the height of the column, a design strategy that aims at the column overdesign could be a viable option for steel open car parks. Moreover, the use of a steel grade S460 revealed to be beneficial in sustaining the applied loads. Finally, the choice of columns made of profiles HE 260 M S460M was the most economical solution.

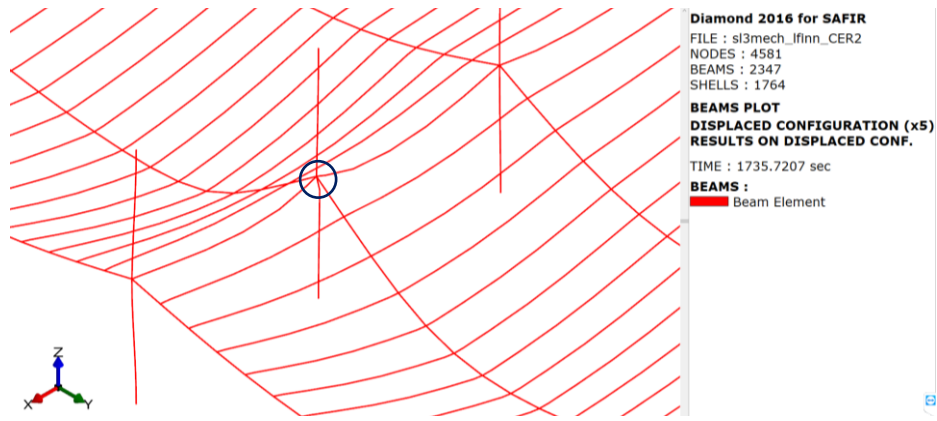
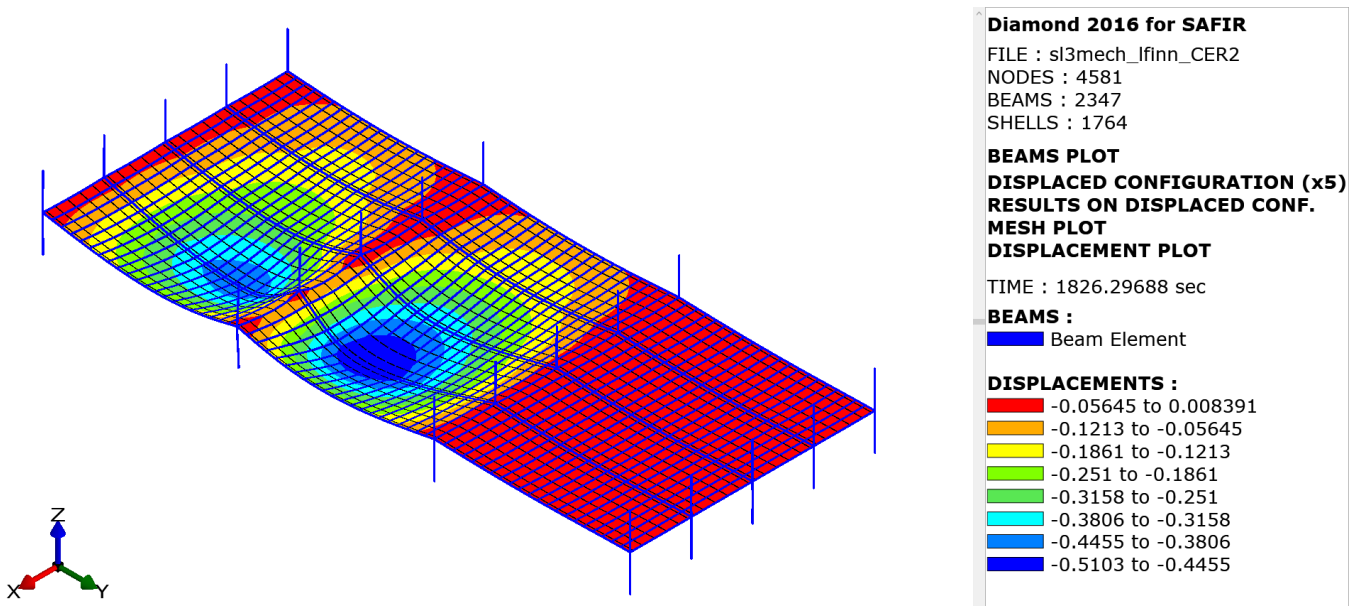
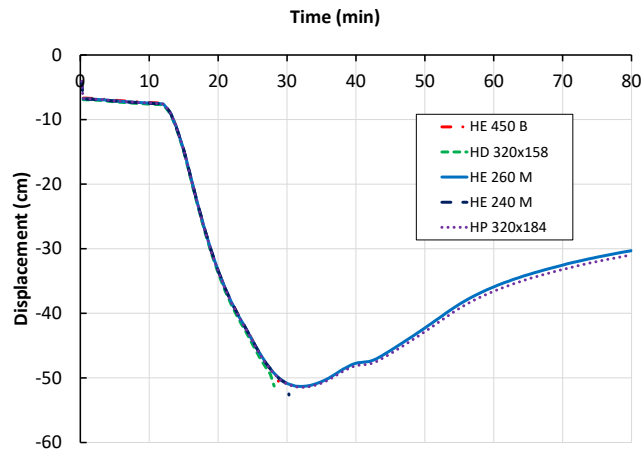


Figure 7. HE 450 B column failure owing to mainly crushing in compression.



(a)



(b)

Figure 8. a) Deformed shape (x5) and vertical displacements (m) of the car park at about 30 min with HE 260 M S460 column; b) maximum vertical displacement evolution of the slab.

## 6 CONCLUSIONS

The paper presented a refined finite element thermo-mechanical of a steel open car park to be built in Italy and subjected to a fire scenario relevant for the column, which is represented by 4 localised fire of burning vehicles that surrounds it. According to a design strategy of the column overdesign, a parametric analysis was performed with the aim to find a suitable bare steel column profile that could satisfy the requirements of structural fire performance by surviving the entire duration of the fire scenario without collapsing. The Hasemi model combined with a newly developed localised fire model, the LOCAFI model, were employed to predict the radiative heat fluxes along the height of the column. The analyses showed that the thermal impact caused by the Hasemi model is much more demanding than the one determined by the LOCAFI model. In particular, failure was attained by mainly crushing in compression of the cross section in the column element just below the ceiling and impacted by the Hasemi model. Moreover, as the axial load was the most significant action on the columns, compact profiles with low section factor, e.g. HE profiles of the M series, are more suitable than profiles with the same cross-sectional area but characterised by more slender flanges and web, e.g. HE profiles of the B series. Finally, an HE 260 M S460M with utilisation ratio of 0.174 in the fire situation was identified as a potential option that could avoid the use partially encased or fireproofed profiles.

## ACKNOWLEDGMENT

This work was supported by the Italian Ministry of Education, University and Research (MIUR) in the frame of the ‘Departments of Excellence’ (grant L 232/2016). Moreover, the information about the structural design provided by design B&V Eng-Arch Office, Corso Novara 99, Turin, Italy, is also acknowledged.

## REFERENCES

1. INERIS (2001) Parcs de stationnement en superstructure largement ventilés. Avis d’expert sur les scénarios d’incendie.
2. EN1991-1-2 (2002) Eurocode 1: Actions on structures – Part 1-2: General actions – Actions on structures exposed to fire, CEN, Brussels.
3. Roosefid M. and Zhao B. (2014) Guide pour la vérification du comportement au feu de parcs de stationnement largement ventilés en superstructure métallique, CTICM.
4. Tondini N., Morbioli A., Vassart O., Lechêne S., Franssen J.-M. (2016) An integrated modelling strategy between FDS and SAFIR: Methodology and application, *Journal of Structural Fire Engineering*, 7 (3), 217-233, [dx.doi.org/10.1108/JSFE-09-2016-015](https://doi.org/10.1108/JSFE-09-2016-015).
5. Vassart O., Hanus F., Brasseur M., Obiala, R., Franssen J.-M., Scifo A., Zhao, B., Thauvoye C., Nadjai A., Sanghoon H. (2016) LOCAFI: Temperature assessment of a vertical steel member subjected to localised fire – Final Report’, Research Fund for Steel and Coal.
6. Tondini N. and Franssen J.-M. (2017) Analysis of experimental hydrocarbon localised fires with and without engulfed steel members, *Fire Safety Journal*, 92:9–22, [dx.doi.org/10.1016/j.firesaf.2017.05.011](https://doi.org/10.1016/j.firesaf.2017.05.011).
7. Tondini N., Thauvoye C., Hanus F., Vassart O. (2019) Development of an analytical model to predict the radiative heat flux to a vertical element due to a localised fire, *Fire Safety Journal*, 105:227-243.
8. Franssen J.-M., Gernay T. (2017) Modeling structures in fire with SAFIR©: Theoretical background and capabilities. *Journal of Structural Fire Engineering*, 8 (3), 300-323.
9. Ministero dell’Interno, D.M. 3 agosto 2015 “Approvazione di norme tecniche di prevenzione incendi”, ai sensi dell’articolo 15 del decreto legislativo 8 marzo 2006, n. 139, Roma, 2015.
10. Gernay T., Millard A., Franssen J.M. (2013). A multiaxial constitutive model for concrete in the fire situation: Theoretical formulation, *Int J Solids Struct* 50(22-23), 3659-3673.
11. Nia S., Gernay T. (2020), Considerations on computational modeling of concrete structures in fire, *Fire Safety Journal*, [10.1016/j.firesaf.2020.103065](https://doi.org/10.1016/j.firesaf.2020.103065).
12. EN 1993-1-2 (2005). Eurocode 3: Design of steel structures - Part 1-2: General rules - Structural fire design, CEN, Brussels.